18 Stellar Evolution: The Rest of the Picture

We'll now consider stellar evolution from the external perspective. All the interior physics is now translated through millions of km of starstuff; Plato's cave doesn't have anything on this. As in Fig. 36 we will still observe stars move through a 2D space as their evolution goes on. But now, instead of T_c and ρ_c (which we can only infer and never directly measure) our new coordinates will be the external observables luminosity and effective temperature, L and $T_{\rm eff}$. In truth even these quantities rely on inference at some level; so while the astrophysicist thinks of (L, $T_{\rm eff}$) the observing astronomer will often think in terms of absolute magnitude (a proxy for L) and photometric colors (a proxy for $T_{\rm eff}$). Yes, we've returned once again to the Hertzprung-Russell diagram first introduced in Sec. 8.

18.1 *Stages of Protostellar Evolution: The Narrative*

The process of star formation is typically divided into a number of separate stages (which may or may not have distinct boundaries). Here, we will consider eight stages, beginning with the initial collapse (which we have already touched on) and ending when a star reaches what is known as the 'main se-

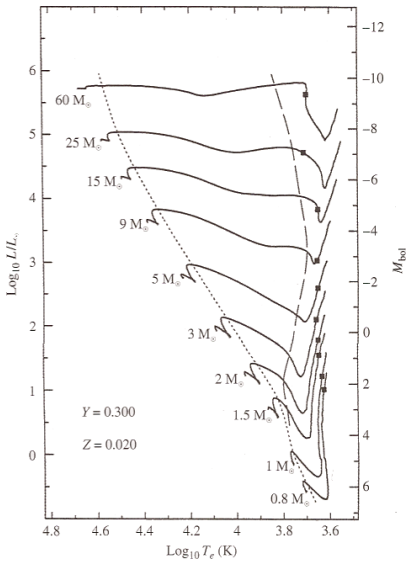

FIGURE 12.11 Classical pre-main-sequence evolutionary tracks computed for stars of various masses with the composition $X = 0.68$, $Y = 0.30$, and $Z = 0.02$. The direction of evolution on each track is generally from low effective temperature to high effective temperature (right to left). The mass of each model is indicated beside its evolutionary track. The square on each track indicates the onset of deuterium burning in these calculations. The long-dash line represents the point on each track where convection in the envelope stops and the envelope becomes purely radiative. The short-dash line marks the onset of convection in the core of the star. Contraction times for each track are given in Table 12.1. (Figure adapted from Bernasconi and Maeder, *Astron. Astrophys.*, *307*, 829, 1996.)

Figure 37:

quence', or a stable state of central nuclear burning of Hydrogen, in which a star will remain for the majority of its life. Note that understanding all of the physics that go into these stages of evolution requires some knowledge of topics we have previously discussed: adiabatic processes (Sec. 11.4), convection (Sec. 12), and opacity (Section7.1) to name a few.

1. **Gravitational Collapse** Initially, the collapse of our Jeans-mass fragment is isothermal: the temperature of the collapsing cloud does not change. The cloud starts at a low density and temperature, and so is optically thin in the infrared, allowing it to efficiently radiate away its collapse energy. However, as the density goes up, the dust grains get closer together until eventually the core becomes optically thick in the infrared, and collapse is halted by the increase in temperature (and thus gas pressure) as the energy from the gravitational collapse is trapped. (Note that theory says that this collapse is an inside-out process: the inner regions collapse faster than the outer regions, and so infall from the collapsing envelope continues during the next few stages). After this point, the core begins to contract nearly adiabatically (as it can no longer exchange heat efficiently with its environment) and continues to heat up as it slowly loses the energy it radiates away. The core will continue to heat up and contract roughly adiabatically, until it reaches a temperature of $\sim$ 2000 K, and some of the energy briefly goes into dissociating all of the H_2 molecules into H, rather than heating the core, causing a second collapse. Once this is finished, the inner region again reaches hydrostatic equilibrium and resumes its slow, adiabatic contraction. This inner object is now referred to as a protostar.

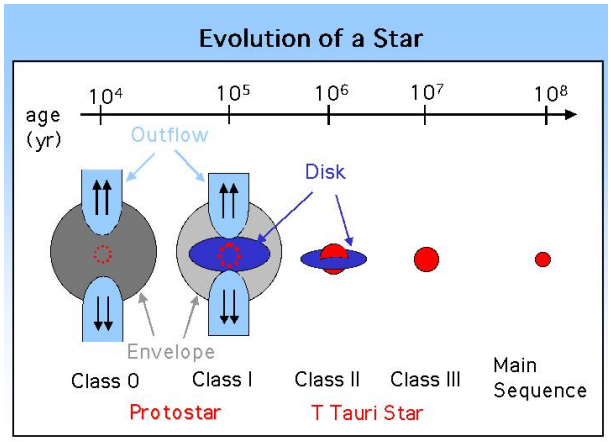

Figure 38: Schematic overview of the early stages of star formation and stellar evolution. (From `http://www-cr.scphys.kyoto-u.ac.jp/research/xray/press200011/figures/`, Apr 2019).

2. **Class 0 protostar** By this stage the envelope may still be collapsing, but a central core has formed which can be seen in cool dust emission at millimeter wavelengths. 'Class 0' is an observational classification indicating that warm dust emission from the core cannot yet be detected at infrared wavelengths. Essentially, the heat generated by the gravitational collapse and accretion has not yet significantly heated a large enough volume of the envelope to destroy the dust, lower the opacity, and make the warm inner regions visible in the infrared. However, there are other observable signatures that show a star is in the process of forming. One key structure that has begun to form at this stage is a flattened, rotating disk. This is a result of the conservation of angular momentum: the smaller the core gets, the faster it spins, causing the initially spherical core to flatten. This actually poses a problem for our forming protostar: if it cannot get rid of this angular momentum, it will never contract to the size of a star, because it would be spinning so fast that it would break up. The solution nature has come up with appears to be bipolar outflows, which begin to be seen at this stage. These rotating flows, launched from the disk (likely with help from the magnetic field, which has also gotten stronger due to conservation of magnetic flux as the cloud collapsed), are believed to carry excess angular momentum away from the system.

3. **Class 1 protostar** In contrast to a Class 0 source, infrared emission from the warm central disk can now be seen. However, material from the envelope is still sufficient to block the protostar from view at optical wavelengths. The outer envelope continues to collapse, infalling onto the central regions. The luminosity that is seen from the central source is largely powered by accretion of this material onto the disk and protostar (this energy comes from a shock, where gas that was in free-fall, traveling at large velocities, suddenly comes to a stop and deposits all of this kinetic energy). The disk continues to drive outflows to remove angular momentum, and by these later stages, now that the disk is larger and better organized, these outflows are better collimated and may even take the form of fast jets.

4. **Classical T-Tauri star (Class 2 protostar)**. The envelope is now sufficiently heated, depleted in mass from infall onto the disk, and/or blown away by the outflows that the central protostar can be seen at optical wavelengths. From this point on the disk will only get smaller as it accretes onto the star and is swept up into planets that are beginning to form. Accretion from the disk remains the primary source of luminosity for the protostar. This accretion is not a continuous process but is extremely stochastic, occurring in large bursts, and so the luminosity of the central object can vary substantially. The 'star' at this point is still much larger than its final radius, and continues to contract. It is also rotating quite quickly at this stage, with rotation periods often around a dozen days (despite its large size), compared to a month for the sun. Its central temperature continues to increase, and though it is still too low for hydrogen fusion, there may be deuterium fusion occurring

(though this does not generate a significant amount of luminosity compared to accretion). T-Tauri stars generally refer exclusively to low mass stars ($\lesssim$ few$M_\odot$). Higher-mass analogues of these systems are known as Herbig Ae/Be stars.

5. **Weak-line T-Tauri star (Class 3 protostar)**. By now, accretion on to the star is almost over (hence, only weak emission lines indicative of hot, accreting gas can be seen in the star's spectrum.) The disk is also only a residual remnant of its former self: exoplanets (especially large gas giant planets) should be well on their way to forming at this point. As the system changes from actively accreting to quiescently contracting, a 'transition disk' may be seen: these objects are expected to have large inner gaps due to planet formation that has cut off the supply of gas to the star, halting its further growth. Remnant disks, which may be mostly rock and dust, having very little gas, can be seen in excess infrared emission from the starlight captured by the dust and reradiated as heat at longer wavelengths. Such debris disks can be understood as massive analogs of the Kuiper belt and zodiacal dust in our own solar system. These disks are observed to persist up to a few million years, telling us how long planets have to form before the raw materials for doing so are used up.

6. **Pre-main sequence star (Hayashi Track).** At some point during the T-Tauri phase, infall stops, and as we can clearly see the central object at optical wavelengths and place it on a Hertzsprung-Russell (HR) diagram (see Fig. 37), we now begin to refer to it as a 'pre-main sequence' star which has reached its final mass (though not yet its final radius). Once the star is no longer getting energy from accretion, its source of energy is just the potential energy released from its gravitational contraction. No matter the energy source, the large size of the star means that it is extremely bright at this point. Although the central star has for some time been too hot for dust to survive, it is still extremely optically thick. The primary source of its opacity is the H^- ion (see Sec. 7.1), which is an extremely temperature-dependent process: it is much more significant at lower temperatures than higher temperatures. The strong temperature dependency of this process causes the star to become convectively unstable throughout. This time, during which the pre-main sequence star is fully convective, in a state of convective equilibrium, and contracting toward its final size, is known as the **Hayashi track**. The star travels a nearly vertical path (nearly constant temperature) on the HR diagram (Fig. 37) until its central temperature becomes high enough for the core to become radiative rather than convective. As previously mentioned for the T-Tauri phase (which may overlap substantially with this phase) the star may already be fusing deuterium.

7. **Henyey Track** (only for stars greater than 0.8 $M_\odot$). Once a star's core becomes radiative, the star executes a sharp leftward turn on the HR diagram (Fig. 37). This occurs because the core is sufficiently hot for the

opacity to drop, which makes convection less efficient, and the core becomes fully radiative. The star reaches a new equilibrium, and depending on its mass, luminosity remains constant or increases slightly (for intermediate-mass stars), and the surface temperature increases slightly or substantially (for massive stars) as it continues to slowly contract. Stars less than 0.8 $M_\odot$ never develop a radiative core, and so reach the main sequence immediately after the Hayashi track. Higher mass stars may spend very little time at all on the Hayashi track before they develop a radiative core and begin moving nearly horizontally across the HR diagram on the Henyey track. At the end of its time of the Henyey track, the star begins nuclear burning. However, as this process is not yet in equilibrium, the star continues to contract, moving down in luminosity toward its final location on the main sequence.

8. **Zero-age Main Sequence.** Once a star reaches the main sequence, it has now begun stable nuclear burning and reached an equilibrium between pressure from this source of energy generation, and gravity. The star will stay here for the majority of its lifetime (millions to billions of years) however, it will continue to slowly change: getting very slightly larger (and so brighter) as it ages. This leads to a famous problem known as the faint young sun paradox: when life on earth was developing, the sun was only $\sim$70% as bright as its current luminosity, however we believe (since life developed) that there was still able to be liquid water on the earth's surface. Although this change in brightness might seem like a good way to determine the age of a star, it turns out that we need to precisely know the mass to do this, and we cannot directly the mass of a star unless it is in a binary system. Outside of stars in clusters (for which we can measure patterns in the positions of more massive stars on the HR diagram that are evolving into red giants), it is difficult to say more than that a star is on the main sequence (which could mean an age of anywhere from a few million to a few billion years!). Some clues can be seen in its spin rate and magnetic activity (both of which decrease), but we are currently limited, at best, to 10-15% accuracy (a fact which, for example, makes it difficult to construct understandings of the time evolution of exoplanetary systems).

18.2 *Some Physical Rules of Thumb*

Let's now dive into a deeper, more physical discussion of the processes involved. Here are a number of key bits we need to worry about:

- **Opacity vs. Temperature**. Fig. 39 gives a schematic view of what we expect here. Roughly speaking, we will have two extremes:

(429) $\kappa_R \propto \rho^{1/2} T^9$ (*below ionization*)

and

(430) $\kappa_R \propto \rho T^{-7/2}$ (*above ionization; Kramer's Rule*).

- **Opacity vs. Thermal Gradient**. If κ is very low, radiation streams freely; otherwise, radiative transport of energy is very inefficient. So in the limit of very high opacity, energy will instead by transported by convection; based on the Schwarzchild stability criterion (Eq. 302) we expect

$$\frac{dT}{dr} = -\frac{T}{P}\left|\frac{dP}{dr}\right|\left(1 - \frac{1}{\gamma_{ad}}\right).$$

  Otherwise, we are in the low-opacity limit and have a radiative profile. By the thermal profile equation (Eq. 12.3) we then expect

$$\frac{dT}{dr} = -\frac{3\rho\kappa L(r)}{64\pi\sigma_{SB}T^3r^2}.$$

- **Virial Theorem.** We saw that stars contract at various stages of their evolution. By Eq. 219, we should also expect that the rate of contraction is limited by a star's ability to radiate energy from its surface.

  1. High opacity $\rightarrow$ convective $\rightarrow$ slow contraction
  2. Low opacity $\rightarrow$ radiative $\rightarrow$ rapid contraction

18.3 *The Jeans mass and length*

A particularly important application of the Virial Theorem, relevant to the earliest stages of star formation, is to determine the conditions required for a system to be slightly out of equilibrium such that it would tend toward

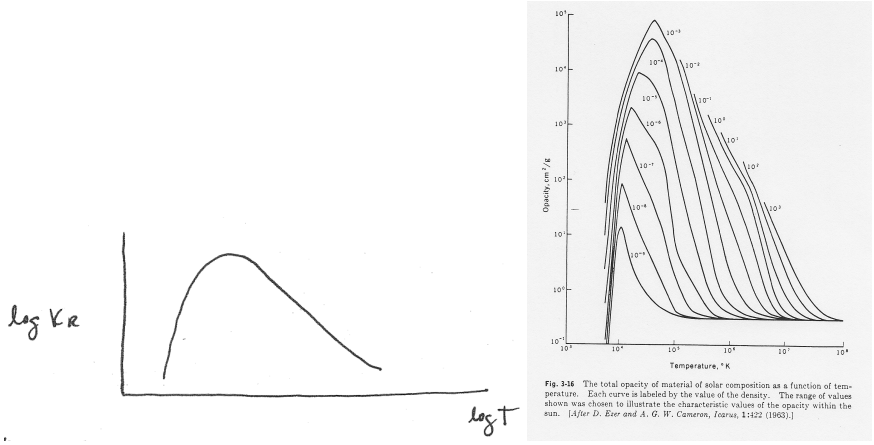

Figure 39: Opacity vs. temperature: *left*, schematic of the Rosseland mean opacity; *right*, an actual calculation (from Ezer and Cameron, 1963).

gravitational collapse or contraction. In this case, we would require that the magnitude of the potential energy term in Equation 209 be larger than the kinetic energy term.

Assuming that we are dealing with an ideal gas, and that we have a spherical, uniform density cloud we can write the total kinetic energy of all the particles in the cloud as

$$K = \frac{3}{2} NkT, \tag{431}$$

where N is the total number of particles in the system. The gravitational potential energy will be the same as Eq. 224,

$$U = -\frac{3}{5}\frac{GM^2}{R}$$

and so we can rewrite the Virial Theorem (Equation 209) as

$$\frac{3}{10}\frac{GM^2}{R} = \frac{3}{2} NkT. \tag{432}$$

the substitutions of $N = M/\bar{m}$ and $R = \left(\frac{3M}{4\pi\rho}\right)^{1/3}$, we can write

$$\frac{1}{5} GM^{2/3} \left(\frac{4\pi\rho}{3}\right)^{1/3} = \frac{kT}{\bar{m}}. \tag{433}$$

Solving Eq. 433 for M gives the mass at which a system will become gravitationally unstable: this is known as the Jeans Mass.

$$M_{\text{Jeans}} = \left(\frac{5kT}{G\bar{m}}\right)^{3/2} \left(\frac{3}{4\pi\rho}\right)^{1/2} \tag{434}$$

We can simplify this equation by scaling it to some typical conditions in the star-forming interstellar medium, and conveniently expressing it in Solar mass units.

$$M_{\text{Jeans}} = 2.3\, M_\odot \left(\frac{T}{10\ \text{K}}\right)^{3/2} \left(\frac{n}{10^5\ \text{cm}^{-3}}\right)^{-1/2} \tag{435}$$

18.4 *Time Scales Redux*

The processes governing each of these stages of stellar evolution are subject to many of the same characteristic time scales that were introduced in Sec. 10.

Collapse and infall

Collapse and infall generally occur on a free-fall time scale (Eq. 198),

$$\tau_{ff} = \sqrt{\frac{3\pi}{32G\rho}}$$

which, as we discussed, is only ∼30 min for the Sun. But before the Sun became a star its density was much lower. If we cast Eq. 198 in more familiar units, we have instead

(436)
$$\tau_{ff} = 2100\text{s} \left(\frac{R}{R_\odot}\right)^{3/2} \left(\frac{M}{M_\odot}\right)^{-1/2}$$

(437)
$$= 0.2\text{yr} \left(\frac{R}{1\text{AU}}\right)^{3/2} \left(\frac{M}{M_\odot}\right)^{-1/2}$$

(438)
$$= 0.6\text{Myr} \left(\frac{R}{0.1\text{pc}}\right)^{3/2} \left(\frac{M}{M_\odot}\right)^{-1/2}$$

So freefall times can be of order 0.1–1 Myr for solar-type stars.

Contraction

Contraction, in contrast, is governed by the time it takes for the star to radiate a significant amount of its gravitational potential energy. This is determined by the Kelvin-Helmholtz time scale (Eq. 205),

$$\tau_{KH} \sim \frac{GM_\odot^2}{R_\odot} \frac{1}{L_\odot}$$

which is roughly 3×10^7 yr for the Sun; longer for lower-mass bodies, and much shorter for more massive stars (see Sec. 10.5).

18.5 *Protostellar Evolution: Some Physics*

First, recall that it is much easier to measure luminosity L (from broadband photometry) and T_{eff} (from spectra) than it is to measure radii. But we can estimate R via Eq. 66,

(439) $L = 4\pi\sigma_{SB} R^2 T_{\text{eff}}^2$.

As we did with the tracks on the T-ρ diagram (Fig. 36), we will also lay out tracks on the H-R Diagram, Fig. 37. For example:

(440) $\log L = 2 \log R + 4 \log T_{\text{eff}} + C$

Hayashi Track Revisited

The key ingredients are are the following. First, once we reach the Hayashi track opacity is high, and the young objects are fully convective. Thus our equation of state is

(441) $P = \frac{\rho k T}{\mu m_p} = K_{con} \rho^{5/3}$

Though contracting, we are still approximately in hydrostatic equilibrium – this is because contraction occurs on $\tau_{KH} > \tau_{ff}$. So we still have

$$\frac{dP}{dr} = -\frac{GM(r)}{r^2}\rho(r) \tag{442}$$

and optical depth is still given by

$$\frac{d\tau}{dr} = -\rho\kappa_R. \tag{443}$$

Combining the above two equations gives

$$\frac{dP}{d\tau} = \frac{GM(r)}{r^2}\frac{1}{\kappa_R} \tag{444}$$

and since temperatures are low at this point the star is mostly neutral and Eq. 429 gives the opacity:

$$\kappa_R \propto \rho^{1/2}T^9.$$

We then solve the above equations for $\tau = 2/3$ and $T = T_{\rm eff}$ (see Sec. **??**). The final solution is that along the Hayashi track (where stars are fully convective because opacity is high), we have

$$\log T_{\rm eff} \approx 0.2\log M + 0.05\log L + C \tag{445}$$

or alternatively,

$$\log L \approx 20\log T_{\rm eff} - 4\log M + C, \tag{446}$$

which matches up fairly well with the nearly-vertical Hayashi track seen on the right-hand side of Fig. 37.

Henyey Track Revisited

As noted above, as the star contracts down the Hayashi track T_c and ρ_c will steadily increase. Eventually, the core will ionize and the opacity will drop (as shown in Fig. 39); as discussed previously in Sec. 12.4 the core will enter the radiative-support regime. At this point L may increase slightly but overall remains fairly constant – all the thermal energy eventually gets out.

With L roughly constant and R decreasing, this means

$$\log T_{\rm eff} = 0.25\log L - 0.5\log R + C \tag{447}$$

must increase. So the star slides to the left along the Henyey Track, leaving the Hayashi Track and heading toward the Main Sequence.

18.6 *Stellar Evolution: End of the Line*

So as we saw when discussing Fig. 36, stellar evolution as seen from the core is a tale of monotonic increases in central ρ and T. From the exterior, it is a story in two parts: each part governed by opacity, ionization, and the transition between convective and radiative interiors.

Once those central ρ and T increases sufficiently, nuclear fusion will begin either via the CNO cycle (for more massive stars) or the p-p chain (for stars of roughly Solar mass and below). In Sec. 15 we already detailed the various nuclear pathways that lead from those earliest stages of fusion to the final endpoints of stellar evolution.

When the central H fuel is finally exhausted, we've seen that the core will contract either until He fusion can be initiated, or until the core becomes degenerate (a He white dwarf). At this point, **shell burning** (Fig. 40) sets in and the star will actually go into reverse, re-ascending along first the Henyey and then the Hayashi track.

Recall that core burning is self-regulating and stable. As a non-degenerate core contracts slightly, its fusion energy production rate will increase dramatically – $\epsilon \propto T^4$ in the pp chain and $\propto T^{16}$ in the CNO cycle. This extra energy

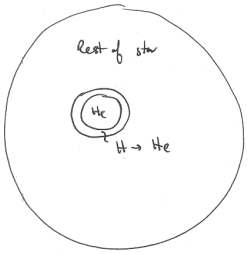

Figure 40: Schematic pictures of shell burning: a degenerate He core surrounded by a thin burning shell surrounded by a mostly-H stellar envelope. Center and left panels are fore an extremely massive star just before the end of its life; Note the linear scales of the two panels.

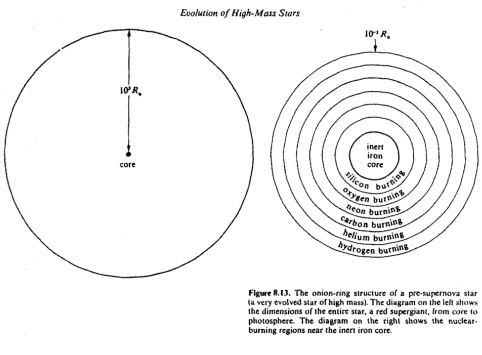

Figure 8.13. The onion-ring structure of a pre-supernova star (a very evolved star of high mass). The diagram on the left shows the dimensions of the entire star, a red supergiant, from core to photosphere. The diagram on the right shows the nuclear-burning regions near the inert iron core.